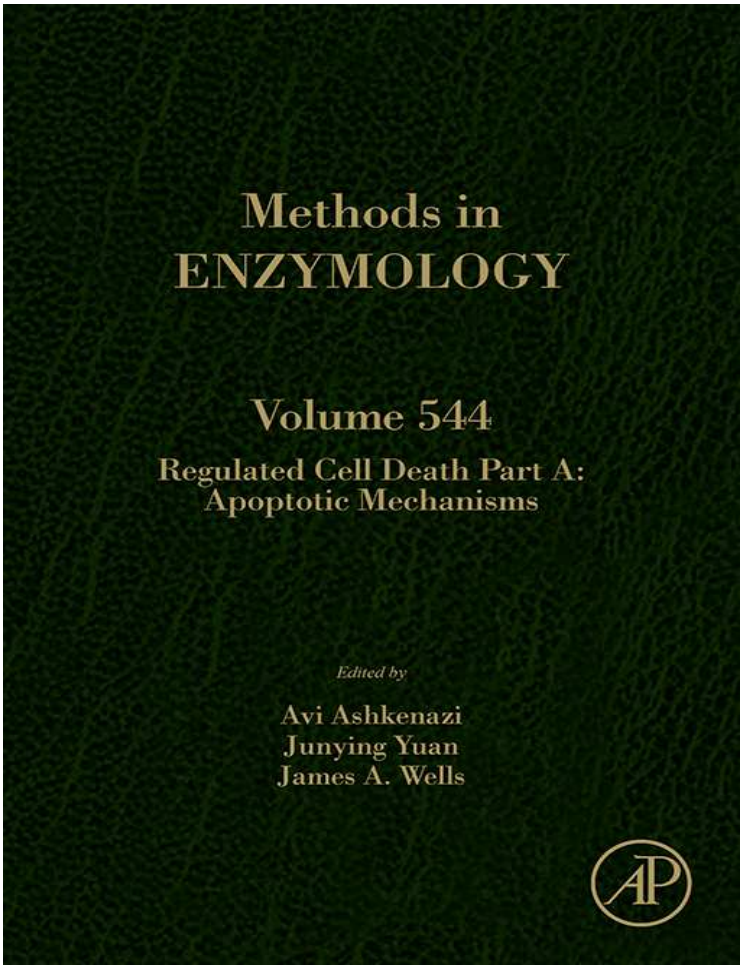

From Kevin Dagbay, Scott J. Eron, Banyuhay P. Serrano, Elih M. Velázquez-Delgado, Yunlong Zhao, Di Lin, Sravanti Vaidya and Jeanne A. Hardy, A Multipronged Approach for Compiling a Global Map of Allosteric Regulation in the Apoptotic Caspases. In: Avi Ashkenazi, Junying Yuan and James A. Wells, editors, *Methods in Enzymology, Vol. 544*, Burlington: Academic Press, 2014, pp. 215-249.
ISBN: 978-0-12-417158-9

CHAPTER NINE

A Multipronged Approach for Compiling a Global Map of Allosteric Regulation in the Apoptotic Caspases

Kevin Dagbay[1], Scott J. Eron[1], Banyuhay P. Serrano[1], Elih M. Velázquez-Delgado[1,2], Yunlong Zhao[1], Di Lin[3], Sravanti Vaidya[4], Jeanne A. Hardy[5]

Department of Chemistry, University of Massachusetts, Amherst, Massachusetts, USA
[1]These authors contributed equally to the work of producing this paper.
[5]Corresponding author: e-mail address: hardy@chem.umass.edu

Contents

[2] Present address: Department of Structural Biology, St. Jude Children's Research Hospital, Memphis, TN, USA.
[3] Present address: College of Pharmacy, Purdue University, West Lafayette, IN, USA.
[4] Present address: Biotechnology Department, MS Ramaiah Institute of Technology, Bangalore, India.

Methods in Enzymology, Volume 544
ISSN 0076-6879
http://dx.doi.org/10.1016/B978-0-12-417158-9.00009-1

Abstract

One of the most promising and as yet underutilized means of regulating protein function is exploitation of allosteric sites. All caspases catalyze the same overall reaction, but they perform different biological roles and are differentially regulated. It is our hypothesis that many allosteric sites exist on various caspases and that understanding both the distinct and overlapping mechanisms by which each caspase can be allosterically controlled should ultimately enable caspase-specific inhibition. Here we describe the ongoing work and methods for compiling a comprehensive map of apoptotic caspase allostery. Central to this approach are the use of (i) the embedded record of naturally evolved allosteric sites that are sensitive to zinc-mediated inhibition, phosphorylation, and other posttranslational modifications, (ii) structural and mutagenic approaches, and (iii) novel binding sites identified by both rationally-designed and screening-derived small-molecule inhibitors.

1. INTRODUCTION

As has been so skillfully outlined in Chapter 7, the apoptotic caspases are central players in both the initiation and execution stages of apoptotic cell death and also function in a number of other biological processes. Due to these roles, control of caspase function is of great interest for applications in medicine, genetic engineering, and developmental biology of multicellular organisms. To date, no caspase-directed therapeutics have successfully emerged from clinical trials. One likely contributor of these failures is that the vast majority of caspase-directed drug candidates to date have targeted the most conserved region of caspases, the active (orthosteric), substrate-binding site. Although the substrate-binding sites of caspases are strongly conserved, other regions of caspases are far less conserved. From a biological perspective, it is quite clear that each caspase is regulated independently from other family members and performs unique roles under various homeostatic conditions due to structural and functional differences that originate away from the active site. It is our view that a more comprehensive and nuanced understanding of the constellations of allosteric[1] regulation of each caspase would not only further our appreciation of the function of each

[1] In this work, we define allosteric as non-active-site regions of the protein.

caspase but would also allow us to select the most effective and selective inhibitory or activating site for uniquely targeting caspases individually.

The central hypothesis of this work is that inhibitors or activators that function at different allosteric sites may yield critical functional differences in cell-based activity, which may ultimately be exploited therapeutically. Evidence for this continues to emerge in caspases, as an exosite required for unique substrate recognition in caspase-7 relative to caspase-3 has recently been discovered (Boucher, Blais, & Denault, 2012). We envision that inhibitors that bind to that site could block a particular subset of cellular caspase-7 substrates. Similarly, the caspase-6 S257D phosphomimetic is catalytically inactive against self-processing and peptide substrates, but can cleave its own prodomain. This suggests that different substrates interact uniquely with caspase-6. Two active-site tetrafluorophenoxymethyl inhibitors with extremely similar biochemical inhibition of caspases-3 and -6 also show very different inhibition of cleavage of mutant huntingtin protein intracellularly (Leyva et al., 2010), further underscoring this idea. Together these observations and the data that are described below suggest that inhibitors that function at different caspase allosteric sites should yield different cellular outcomes, which should prove to be therapeutically useful.

Allosteric drugs, in general, are proving to be an effective means for achieving selectivity within families of highly related proteins. To date, the vast majority of allosteric sites used were discovered by chance. In this chapter, we describe a multipronged approach that we have developed and are using in an ongoing way to identify the full spectrum of allosteric regulation that is applicable in the apoptotic caspases. We envision that the same approach that we describe may also be applicable in other protein families, which is an additional motivation for this chapter. Here we describe how we combine the information encrypted in the record of naturally evolved allosteric sites that can be accessed by interrogating posttranslationally modified caspases, zinc-inhibited forms of caspases, mutagenic studies, and the interactions of both novel and known chemical ligands to produce a comprehensive map of caspase allostery. The current map of caspase allostery (Fig. 9.1) combines data from our work with data from many other labs and has identified at least seven nonoverlapping allosteric sites on various caspases. The emerging themes from this work are (1) various caspases are differentially regulated by the same chemical signals (e.g. zinc, phosphorylation), (2) many different sites within the caspase catalytic core domain are sensitive to regulation, and (3) indirect allosteric control of the loops that compose the active site by many inputs modulates caspase function.

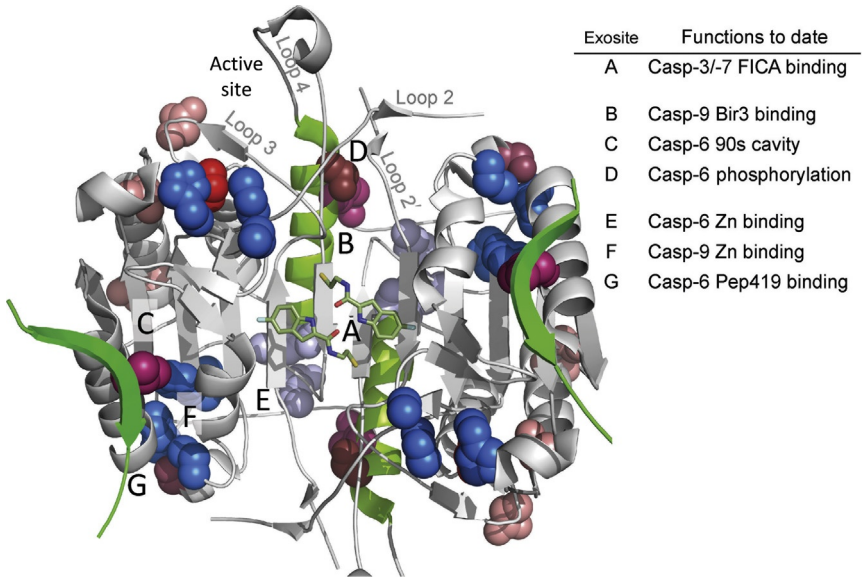

Figure 9.1 Current map of global apoptotic caspase allostery. Exosites that have been identified by the methods included in this chapter are annotated on a canonical caspase structure (gray cartoon). Red, phosphorylation; blue, zinc binding; green, chemical ligands. Various shades of red are used to denote sites of phosphorylation in different caspases. The green caspase helix that forms exosite B is highlighted in the chemical ligands to indicate that this is the region that interacts with the BIR3 region of XIAP- and BIR3-derived peptide inhibitors. *Adapted from Velazquez-Delgado (2012) with permission.*

2. ZINC-MEDIATED ALLOSTERIC INHIBITION OF CASPASES

Inhibition of caspases by zinc was reported soon after the discovery of caspases (Chimienti, Seve, Richard, Mathieu, & Favier, 2001; Schrantz et al., 2001; Stennicke & Salvesen, 1997). Until recently, the molecular details and sites of inhibition were not known. We have shown that each apoptotic caspase has unique metal-binding and inhibition profiles (Huber & Hardy, 2012; Velazquez-Delgado & Hardy, 2012b). Caspases-6 and -7 each bind just one zinc per monomer, whereas caspase-9 binds two zincs (Huber & Hardy, 2012) and caspase-3 binds three zincs (Velazquez-Delgado & Hardy, 2012b). Caspase-6 binds zinc only at exosite E (Fig. 9.2A), but not at the active site (Velazquez-Delgado & Hardy, 2012b). Thus, understanding metal-binding preferences provides insights

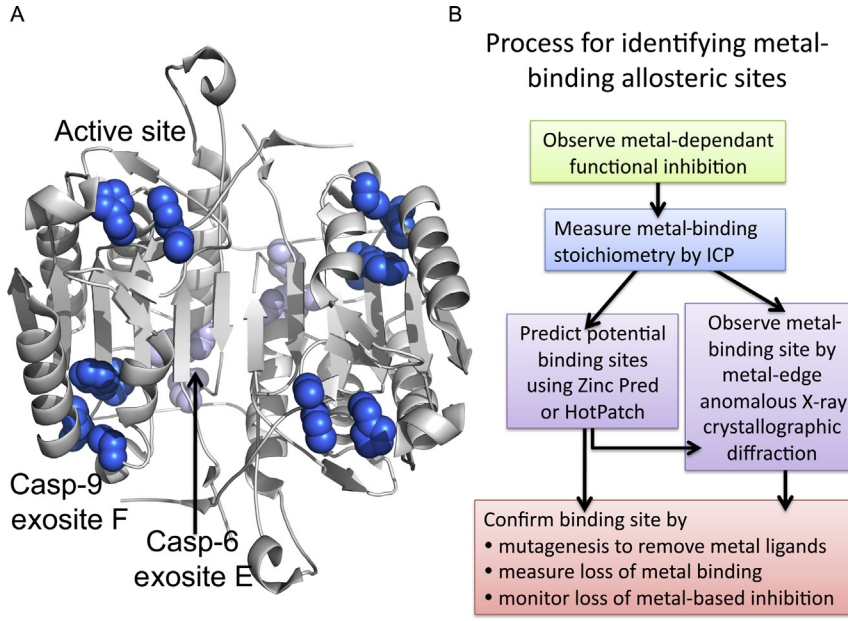

Figure 9.2 Discovery of zinc-binding sites in caspases. (A) Exosites for zinc binding that have been identified to date are shown as spheres on a canonical caspase structure (cartoon). The caspase-9 active site is capable of binding zinc; however, the active site of caspase-6 is not the dominant zinc-binding site in the unliganded protein. Caspase-6 is inhibited by zinc at exosite E. (B) Flowchart enumerating the methods used to identify metal-binding exosites and their mechanisms of allosteric inhibition in caspases. *(A) Adapted from Velazquez-Delgado (2012) with permission.*

into mechanisms that can be exploited to achieve caspase-specific inhibition, so long as the preferences are understood for all related caspases. The process of utilizing zinc binding to define allosteric sites (Fig. 9.2B), described in Sections 2.1 and 2.2, utilizes widely available approaches that are applicable for all caspases as well as for virtually any other protein in which the inhibition by zinc or other metals has been observed.

To date, no clear biological role for zinc-mediated regulation of caspases has been reported; nevertheless, the currently available data suggest that zinc may play a role in regulation of apoptosis. The life–death balance in the cell is tightly coupled to zinc levels. It is becoming increasingly clear that zinc is a critical cellular regulator that some suggest may play roles as significant for cellular homeostasis as calcium is to signal transduction (for review, see Fukada & Kambe, 2011). Even the smallest fluctuation in cellular zinc concentration appears to tip a cell toward survival or apoptotic cell death

(Zalewski, Forbes, & Betts, 1993), which could be in part due to the role of zinc-mediated inhibition of caspases (Perry et al., 1997; Stennicke & Salvesen, 1997). Moreover, controlling zinc levels has been harnessed in several biological contexts. The pathogenic bacterium *Helicobacter pylori* sequesters and then releases zinc into infected cells, inhibiting caspase activity and avoiding apoptotic cell death (Kohler et al., 2010, 2009). These data may be consistent with a model in which at low zinc levels, zinc-mediated inhibition of caspases is released, allowing apoptosis to be induced. Patients with asthma and chronic bronchitis are prone to zinc deficiency leading to increased levels of apoptosis in airway epithelium (Carter et al., 2002; Truong-Tran, Grosser, Ruffin, Murgia, & Zalewski, 2003). PAC-1 is a serendipitous small-molecule procaspase-3 activator which does not directly activate procaspase-3 (Denault, Drag, et al., 2007) but works by relieving zinc-mediated inhibition (Peterson et al., 2009), showing that zinc-mediated inhibition of caspases may be therapeutically exploited. Although physiologically "free" or unliganded zinc concentrations are reported to be in the femto- to picomolar range (Bozym, Thompson, Stoddard, & Fierke, 2006; Krezel & Maret, 2006), the "available" zinc pool appears to be much higher. Eukaryotic cells contain $\sim$200 μM zinc (Krezel & Maret, 2006) where small shifts in glutathione concentration or oxidative stress release zinc from the metallothioneins (Krezel, Hao, & Maret, 2007) or secretory vesicles. Although it is too early to conclude that zinc plays a significant physiological role directly in caspase regulation, it is possible that dissecting the relationship of zinc and caspases may itself be therapeutically relevant, in addition to its utility in defining the allosteric map for caspases described here.

2.1. Allosteric site identification in caspase-9 using metal-binding site prediction algorithms

Caspase-9 is inhibited in the core domain by zinc but not by other metals (Fig. 9.3A; Huber & Hardy, 2012) and binds two zincs per monomer (Huber & Hardy, 2012). We predicted eight putative zinc-binding sites by combining HotPatch and PREDZINC analysis with visual inspection of the caspase-9 structure. Mutagenesis of the true zinc ligands prevented zinc binding (as measured by inductively coupled plasma–optical emission spectroscopy (ICP–OES)), whereas mutagenesis of the other sites had no effect on zinc binding. Zinc binds to the caspase-9 active site as well as to exosite F comprising C230, H224, and C272 (Huber & Hardy, 2012) (Fig. 9.3B). Zinc binding to the active site is the primary site of inhibition,

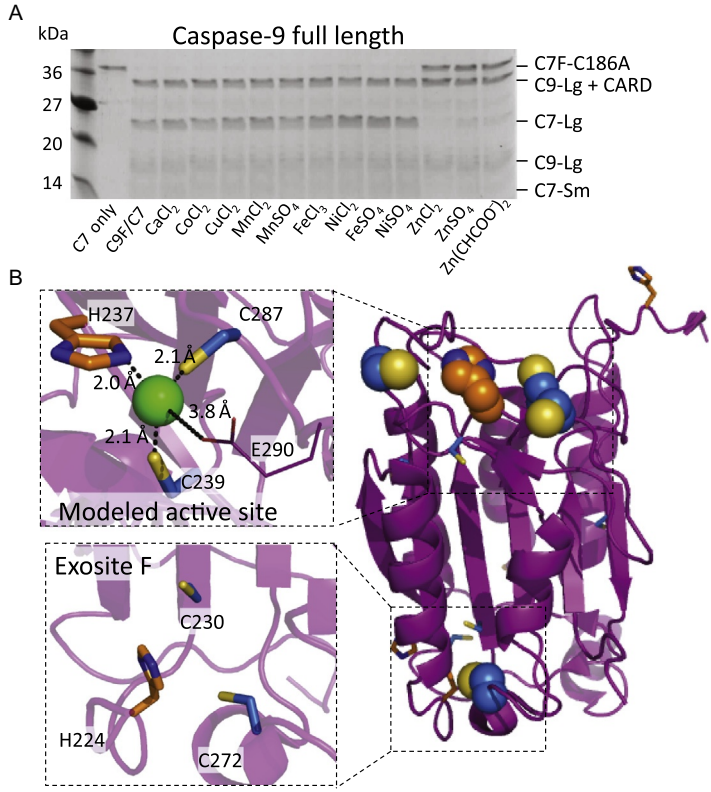

Figure 9.3 Zinc binds and inhibits both active and allosteric sites in caspase-9. (A) Zinc is the predominant metal cation to inhibit full-length caspase-9 (C9 FL) as monitored by cleavage of a natural caspase-9 substrate, the caspase-7 zymogen (C7 C186A) to the caspase-7 large (C7-Lg) and small (C7-Sm) subunits. (B) Location of the conserved active-site and exosite-ligand clusters on caspase-9 (PDB ID 1JXQ). A model of caspase-9 active-site ligand interactions with a modeled zinc ion was obtained by altering the H237, C239, and C287 rotamers in PyMol. *Adapted from Huber and Hardy (2012) with permission.*

since the K_i for zinc when exosite F is ablated ($5.0 \pm 2.8\ \mu M$) is similar to that of WT caspase-9 ($1.5 \pm 0.3\ \mu M$). Detailed kinetic analysis shows a mixed mode of inhibition, which suggests that exosite zinc binding is also involved in inhibition and indicates that exosite F should be categorized as a functional allosteric site. Given the ligand sphere identified, we generated a model of zinc binding to caspase-9 (Fig. 9.3B). Three of the four zinc-liganding residues in exosite F are conserved across the caspase family, but we have shown that caspase-6 does not bind zinc at exosite F (Velazquez-Delgado & Hardy, 2012b). This suggests that exosite F may require all four

zinc ligands to robustly bind zinc and may therefore not be functional in other caspases, making it unique to caspase-9. This approach using zinc-binding site prediction coupled with mutagenesis can also feed into the methods outlined in Section 2.2 (Fig. 9.2), provided the zinc-anomalous diffraction experiment is technically feasible.

2.2. Allosteric site identification in caspase-6 using X-ray crystallography with anomalous diffraction

Caspase-6 is inhibited by zinc but not by other transition metals tested (Fig. 9.4A) (Velazquez-Delgado & Hardy, 2012b). Using ICP–OES to quantify zinc, we observed that each inhibited caspase-6 monomer bound just one zinc (Fig. 9.4B). To identify the ligands composing the zinc-binding site, we soaked crystals of caspase-6 with zinc and then performed an anomalous diffraction experiment with X-rays tuned at the zinc edge. Anomalous X-ray diffraction is a robust method for unambiguously locating metal-binding sites as only those atoms that diffract anomalously are observed at high intensity. One peak (5σ) per monomer was observed in the zinc-anomalous map (Fig. 9.4C). This site is composed of three liganding residues, K36, E244, and H287, and one water molecule. Removal of any of these ligands prevents zinc binding as assessed by ICP–OES (Fig. 9.4B), further validating the location observed in the anomalous X-ray diffraction experiment. E244 makes a bidentate interaction with the zinc, which exists in a distorted tetrahedral geometry. Lysine residues are uncommon but not unheard of ligands for zinc. In fact, 3% of zincs present in structures in the protein data bank use lysine as a ligand. Given that this preferred site in caspase-6 utilizes lysine as a ligand, we can envision that a site such as this could be overlooked by prediction algorithms, making anomalous X-ray diffraction combined with ligand removal by mutagenesis the preferred method for identifying zinc-sensitive allosteric sites. A structure-based sequence alignment indicates that exosite E is not present in any of the other caspases. Inhibition for the exosite E mutants (K36A, E244A, H287A) by zinc is much weaker than the WT suggesting that although zinc may be able to inhibit caspase-6 at the active site, exosite E is the predominant inhibitory site. Most importantly, no zinc is observed bound to caspase-6 at low or neutral pH when exosite E is knocked out. This result demonstrates that caspase-6 exists in the helical conformation, wherein the 120's and 60's regions are converted from strand or loop to helix. This helical conformation is observed for apo caspase-6 (Baumgartner et al., 2009; Vaidya, Velazquez-Delgado, Abbruzzese, & Hardy, 2011). In this helical

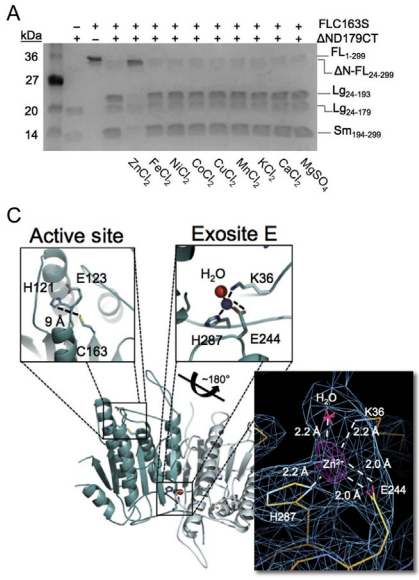

B

	Zinc : Monomer
Caspase-3 (Wild type)	3.2 ± 0.4
Caspase-6 (Wild type)	1.0 ± 0.2
Active site C163S	0.8 ± 0.1
Exosite E K36A	0.4 ± 0.1
E244A	0.4 ± 0.3
H287A	0.2 ± 0.2
E244A/H287A	0.3 ± 0.2
Exosite F H108A/C148A	1.2 ± 0.3
Caspase-7 (Wild type)	0.7 ± 0.1
Caspase-9 (Wild type)	1.8 ± 0.3
Active site C287A	0.8 ± 0.1
H237A	0.8 ± 0.1
C287A /C239S	0.7 ± 0.3
Exosite F C272A	0.7 ± 0.3
Active + F C272A /C287A	0.2 ± 0.2

Figure 9.4 Zinc binds an allosteric site to inhibit caspase-6. (A) Metal inhibition was tested in an electrophoretic mobility gel-based assay as fragments produced from active caspase-6-(ΔND179CT) mediated cleavage of the full-length C163S zymogen (substrate). Fragments from cleavage include the following: full length (FL), FL lacking the N-terminal prodomain (ΔN-FL), large (Lg), and small subunits (Sm) with the amino acids present in those bands (subscripts) labeled. Zinc is the only metal cation that inhibits caspase-6 activity. (B) The zinc-binding stoichiometry for various caspases, as well as mutants designed to ablate zinc binding are shown. Zinc binding was measured by inductively coupled plasma–optical emission spectroscopy. (C) The structure of zinc-bound caspase-6 (ribbons, PDB ID 4FXO). An anomalous difference map calculated from data collected above the zinc absorbance edge is contoured at 5σ (inset, purple mesh), clearly indicating the location of zinc at the allosteric site (black inset). The side chains and water serving as ligands are drawn as sticks. The 2Fo-Fc electron density map (blue) into which the structure was build is contoured at 1σ. The boxed regions show active site, which contains residues appropriate for metal binding including H121, E126, and C163. In this structure, these residues are not properly positioned to coordinate zinc. The caspase-6 zinc-binding exosite is shown with the side chain ligands for zinc in sticks (K36, E244, H287), zinc (blue), and the water molecule (red). *Adapted from Velazquez-Delgado and Hardy (2012b) with permission.*

conformation, the active-site liganding residues H121 and C163 are too far apart to robustly bind zinc (Fig. 9.4C) at both low and neutral pHs. Zn inhibits caspase-6 by locking the enzyme into the inactive helical conformation (discussed at greater length in Section 5.2). We envision that similar

zinc-binding allosteric sites may exist on a wide number of proteins, given that up to 10% of proteins are functionally sensitive to zinc (Fukada & Kambe, 2011). The methods outlined here (inhibition and ICP studies combined with mutagenesis of zinc-liganding side chains and structure determination with anomalous diffraction tuned at the zinc edge) should be applicable to the study any of these zinc-sensitive sites.

3. USING THE EMBEDDED RECORD OF FUNCTIONALLY IMPORTANT POSTTRANSLATIONAL MODIFICATIONS TO IDENTIFY ALLOSTERICALLY SENSITIVE SITES

The majority of posttranslational modifications (PTMs) occur because they play a functional role in the modified protein (Minguez et al., 2012; Seet, Dikic, Zhou, & Pawson, 2006). Many examples of PTMs inducing protein–protein interactions or altering substrate recognition which mediate many other crucial signaling pathways exist. Like many proteins, caspases are posttranslationally modified. In addition to proteolytic cleavage (zymogen activation), caspases are also phosphorylated, nitrosylated, ubiquitinated and glutathionylated in a manner that impacts function. We have seen that probing the way that nature has exploited functionally sensitive sites by PTM is a useful means of uncovering new allosteric sites.

3.1. Phosphorylation in apoptotic caspases

Caspases and kinases work in concert to regulate one another in a complex, intertwining web. Many caspases, including the apoptotic caspases-2, -3, -6, -7, -8, and -9, have been reported to be extensively phosphorylated, typically leading to inactivation and avoidance of apoptosis. In the active state, caspases often cleave and inactivate the very kinase that phosphorylates them. Caspases are highly phosphorylated and the sites and impact of phosphorylation continue to be reported (for review, see Kurokawa & Kornbluth, 2009; Lopez-Otin & Hunter, 2010). There are a large number of ongoing studies to map the caspase–kinase interplay. For example, the Cravatt lab recently completed a comprehensive mapping of phosphorylation and caspase cleavage (Dix et al., 2012). Some sites of phosphorylation directly block sites of autoprocessing or cleavage by upstream caspases (Duncan et al., 2011), but most others appear to lead to caspase inactivation. Thus, many of the sites of caspase phosphorylation are an embedded historical record of sensitive sites from which caspase function can be activated or inhibited.

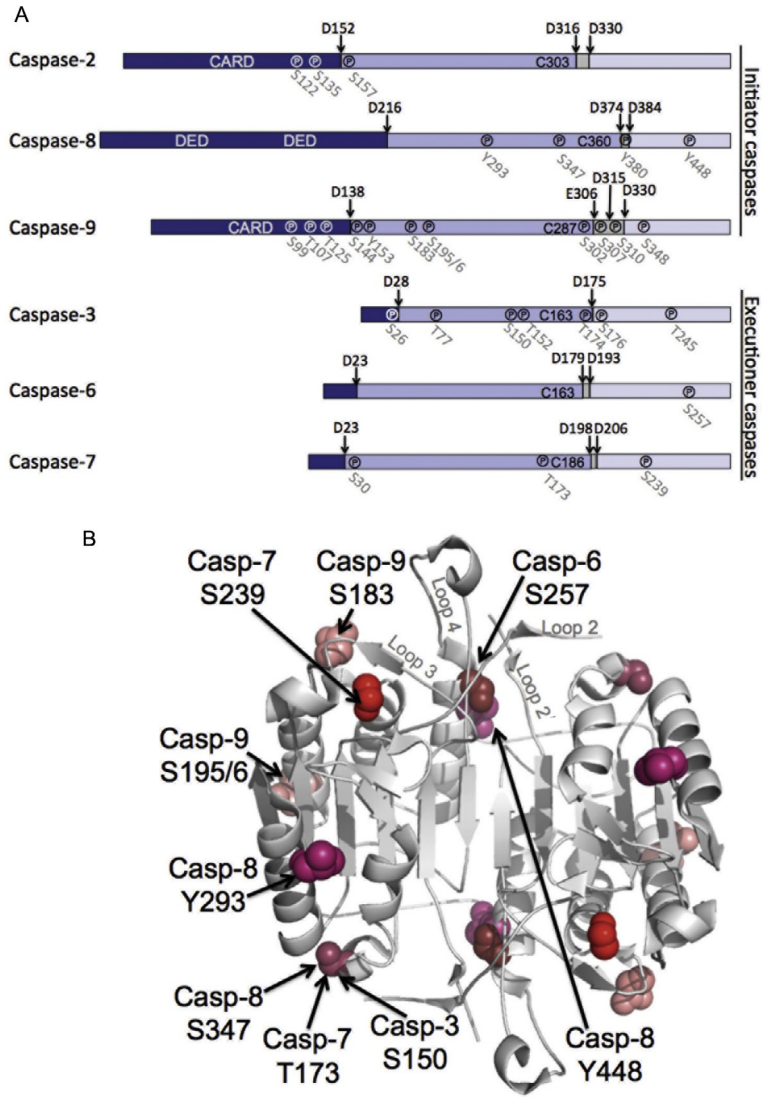

Figure 9.5 Confirmed sites of phosphorylation in apoptotic caspases. (A) This map represents the major, confirmed sites of phosphorylation in the apoptotic caspases. We recognize that some other sites of phosphorylation have been reported in various databases. (B) Structural distribution of functionally critical sites of phosphorylation. *(A) Adapted from Velazquez-Delgado and Hardy (2012a) with permission. (B) Adapted from Velazquez-Delgado (2012) with permission.*

A large number of sites of phosphorylation have been identified to date (Fig. 9.5A and B); however, in many cases, the exact biological conditions that lead to phosphorylation and the extent to which particular sites are phosphorylated have not yet been extensively studied. So far, three

PAK-2 sites: T77, T152, and T245 in caspase-3 and three sites: S30, T173, and S239 in caspase-7 were identified via peptide-based mapping (Li et al., 2011). In neutrophils, caspases-3 and -8 are phosphorylated by p38 MAPK at S150 and S347, respectively (Alvarado-Kristensson et al., 2004). S257 was the confirmed phosphorylation site of caspase-6 (Suzuki et al., 2004). Three more phosphorylation sites in caspase-3, S26, T174, and S176, are adjacent to the cleavage sites in the caspase-3 prodomain and intersubunit linker (ISL) (Dix et al., 2012; Duncan et al., 2011). In addition to the single serine phosphorylation on caspase-8, S347, there are three tyrosine phosphorylation sites at Y293, Y380, and Y448 (Jia, Parodo, Kapus, Rotstein, & Marshall, 2008). Research in neutrophils indicates that an intense competition occurs between these sites. The winner decides the fate of the cell by either maintaining the inhibited state or activating apoptosis. Both Y380 and Y448 are phosphorylated by the Src tyrosine kinase Lyn, which results in resistance to activational cleavage and thus a dearth of caspase-8-mediated apoptosis. However, phosphorylation on Y293 is reported to stimulate an interaction with the phosphatase SHP-1, which then dephosphorylates caspase-8 and allows for apoptosis to proceed.

To date, caspase-9 appears to be the most heavily phosphorylated caspase, with 12 known phosphorylation sites variously recognized by 9 different kinases. This complex regulatory system spans the entirety of the protein, including phosphorylation sites on the caspase activation and recruitment domain (CARD), the large and small subunits, as well as the ISL. The most studied phosphorylation event occurs at T125, which is modified by four different kinases: ERK1, ERK2, DYRK1A, and CDK1. Phosphorylation at T125 results in the inability of caspase-9 to be activated (Allan & Clarke, 2007; Allan et al., 2003; Seifert, Allan, & Clarke, 2008) and thus a suppression of apoptosis. This has been linked to cancer and tumorigenesis, with specific implications of this phosphothreonine as a hallmark for gastric carcinomas (Yoo, Lee, Jeong, & Lee, 2007). In addition, three other kinases, Akt, PKA, and PKCζ, phosphorylate caspase-9 and lead to inactivation, stifling cell death. In contrast to these inhibitory effects, it is reported that the kinase c-Abl phosphorylates caspase-9 and promotes autoprocessing (Raina et al., 2005). It was observed that c-Abl phosphorylates caspase-9 at Y153 after exposing the cell to DNA-damaging agents. The results indicated an enhancement of caspase-9 autoprocessing and acceleration of apoptosis after genotoxic stress. Given that the vast majority of phosphorylation sites in caspases lead to a change in function, by examining

sites that are phosphorylated (Fig. 9.5), we can come to understand divergent mechanisms of allosteric regulation that can be exploited within this family.

3.2. Mechanism of phosphorylation-based allosteric caspase-6 inhibition

Only one site of phosphorylation, S257, has been reported to date for caspase-6. ARK5 kinase phosphorylates caspase-6 S257 (Fig. 9.5A), leading to inactivation (Suzuki et al., 2004). Given that this residue is not in the active site or substrate-binding groove, we hypothesized that this phosphorylation constituted a natural mechanism of allosteric regulation. Our work (Velazquez-Delgado & Hardy, 2012a) was reported nearly concurrently with another study of S257 phosphorylation (Cao et al., 2012). These two papers were the first to provide any structural detail of how phosphorylation leads to inactivation of any caspase. To understand the mechanistic details of allosteric inactivation at this site, both groups utilized a phosphomimetic approach, in which S257 was replaced by Asp (S257D) (Velazquez-Delgado & Hardy, 2012a) or Glu (S257E) (Cao et al., 2012). Both Glu and Asp have been successful phosphomimetics, as the length and charge are similar to phosphoserine. S257D is a robust phosphomimetic that is inactive, similar to caspase-6 phosphorylated by purified ARK5 kinase (Fig. 9.6A). By subjecting the phosphomimetic to limited proteolysis by caspases-3, -6, or -9, we observed that the active-site loops were ordered differently from the wild-type (WT) enzyme (Fig. 9.6B). To visualize the newly ordered active-site loop bundle, we determined the crystal structure of caspase-6 S257D. The crystal structure of caspase-6 S257D suggests that phosphorylation of S257 inactivates caspase-6 through a steric clash with a single residue, P201, in the L2′ loop (Velazquez-Delgado & Hardy, 2012a) (Fig. 9.6C and E). This steric clash causes the L2′ loop to be dramatically reordered into the inactive down position (Fig. 9.6C). The phosphomimetic S257D is dramatically inactivated with a k_{cat}/K_M that is three orders of magnitude lower than WT (Fig. 9.6D). S257E is also dramatically inactivated relative to WT (Cao et al., 2012). Substitution of S257 with uncharged but large residues also leads to inactivation, suggesting that charge is not critical to the mechanism of inhibition. Removal of the clashing proline side chain by the P201G substitution relieves the inhibition (Fig. 9.6D and E), demonstrating that steric clash is responsible for the phosphorylation-mediated inhibition of caspase-6. Thus, it is clear that phosphomimetic versions of caspases are a powerful method for

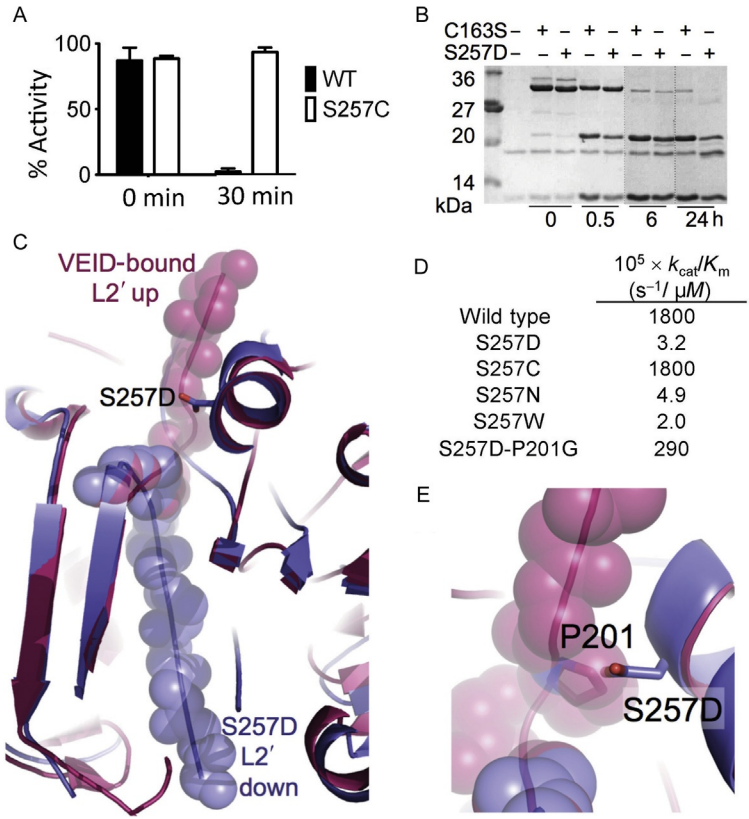

Figure 9.6 S257D is a robust phosphomimetic that elucidated the mechanism of allosteric inhibition by phosphorylation. (A) WT caspase-6 is inhibited by 30 min incubation with ARK5 kinase, whereas the S257C unphosphorylatable mutant is unaffected by ARK5. The S257D phosphomimetic is inactive similar to phosphorylated WT caspase-6. (B) The S257D active-site loops are ordered differently from the C163S zymogen, leading to different rates of cleavage of S257D from C163S. (C) In the structure of S257D (PDB ID 3S8E), the L2′ loop is in a down position (inactive, blue) in contrast to the VEID (substrate)-bound structure in which the L2′ loop is in the up position (active, red). (D) Mutations at S257 show that size is more important than charge in S257 inhibition and that any residue larger than cysteine or serine results in inactivation. Removal of P201 by mutation to glycine restores activity to S257D indicating that a steric clash between P201 and S257D leads to loss of activity. (E) The steric clash between P201 and S257D mirrors that of phosphoserine 257. *Adapted from Velazquez-Delgado and Hardy (2012a) with permission.*

understanding how phosphorylation leads to structural and functional changes allosterically. Because this site has not been reported to be phosphorylated in other caspases, this particular site seems to be unique to caspase-6. Close inspection of sites of phosphorylation in other caspases lead

us to predict that this region may be ripe for allosteric regulation by phosphorylation by other kinases. For example, in caspase-8, the Y448 site in the same region (Fig. 9.5B) is phosphorylated by Lyn kinase leading to inactivation (Jia et al., 2008).

3.3. Other PTMs that allosterically regulate caspases

While phosphorylation of caspases has been extensively reported, other PTMs, which mediate many other crucial signaling pathways, also occur on caspases to regulate structure, function, translocation, or interactions with other proteins, sometimes in an allosteric manner.

To date, no robust proteomics analysis to identify the global PTMs in caspases has been reported. Although the current list of caspase PTMs has been compiled in a case-by-case manner, a significant number of PTMs that are related to the oxidation of cysteine have been identified. As cysteine proteases, caspases are sensitive to redox signaling, so cellular oxidative stress provides an abundant source for functional PTMs at thiol groups in caspases. Nitric oxide was first reported to be able to directly inhibit caspases-1, -2, -3, -4, -6, -7, and -8 through S-nitrosylation and thereby inhibit apoptosis (Dimmeler, Haendeler, Nehls, & Zeiher, 1997; Kim, Talanian, & Billiar, 1997; Li, Billiar, Talanian, & Kim, 1997). Recently, the S-nitrosylation site in caspase-3 was identified to be the catalytic cysteine C163 in nitrite-treated endothelial cells (Lai et al., 2011). GSSG is another oxidative agent with dose-dependent behavior that inhibits caspase-3 activity via protein glutathionylation at the catalytic cysteine and C220 in helix 4 (Huang, Pinto, Deng, & Richie, 2008). It is of note that oxidizing PTMs are usually reversible and sensitive to reducing agents. Both denitrosylation and deglutathionylation were observed in DTT-treated samples with a resulting restoration of caspase-3-like activity (Huang et al., 2008; Li et al., 1997).

Although the primary mode of inhibitory redox-sensitive PTMs is to directly ablate the nucleophilicity of the catalytic cysteine (e.g., caspase-3 C163), other cysteines in caspases are modified. Caspase-3 C220 is a known secondary glutathionylation site (Huang et al., 2008), but there are other solvent-accessible cysteines that could be alternate PTM sites. At least three cysteines in caspase-3, for instance, are located in regions that are significant to caspase function. C264 (caspase-7 C290, see Section 4.1) is located at the dimer interface where modification can lead to inhibition or activation. Other possible mechanisms of inhibition we may expect to observe include

PTM influencing the orientation of the active-site loops at a distance as we have seen for small-molecule caspase modulators (see Section 4.1). Both C148 which is at the bottom of a helix and C184 in the L2 loop are located near a region that could make electrostatic interactions with the active-site loop bundle. Whether any of these sites could become potential targets for redox-related PTMs and contribute to an allosteric inhibition of caspases is still awaiting further elucidation. As an example of allosteric inhibition using redox PTM, the engineered "handcuff-like" disulfide bond locks caspase-7 in to the inactive apo-conformation under oxidative conditions when a reactive cysteine pair that was introduced across the dimer interface of caspase-7 is oxidized (Witkowski & Hardy, 2011).

In addition to the redox-sensitive sites, one functionally relevant nonredox PTM has been reported. In contrast to other caspases, caspase-8 activity is enhanced by polyubiquitination because it forms an aggregate with p62, a polyubiquitin-binding protein, and increases the stability of cleaved caspase-8 which enhances proteolytic activity (Jin et al., 2009). In addition, sumoylation of caspase-7 has been reported, which appears to impact nuclear localization of caspase-7 (Hayashi, Shirakura, Uehara, & Nomura, 2006).

4. SYNTHETIC SMALL-MOLECULE INHIBITORS TO IDENTIFY ALLOSTERIC SITES

Synthetic chemical ligands have proven to be one excellent source of new information about novel allosteric sites in proteins (for review, see Hardy & Wells, 2004), conformational flexibility within proteins, and biological roles of enzymes. In caspases, the use of disulfide tethering, a method of site-directed ligand discovery (Erlanson et al., 2000; Erlanson, Wells, & Braisted, 2004), led Jim Well's group at Sunesis Pharmaceuticals to identify the first allosteric site in caspases-3 and -7 (Hardy, Lam, Nguyen, O'Brien, & Wells, 2004a) (exosite A, Fig. 9.7). Additional ligands that inhibited the inflammatory caspase-1 at the same site were discovered soon after (Datta, Scheer, Romanowski, & Wells, 2008; Scheer, Romanowski, & Wells, 2006), and this site continues to be a target of new small-molecule pan-caspase inhibitors (Feldman et al., 2012). Inhibition of procaspase-3 by zinc was defined upon exploration of the mechanism of activation by the chemical ligand PAC-1 (Peterson et al., 2009) which directly competes with the caspase-3 active site for zinc. We have shown that synthetic peptide ligands can be used to modulate dimerization of caspase-9 (Huber, Ghosh, & Hardy, 2012) (exosite B, Fig. 9.7) and a small peptide, Pep419, has been

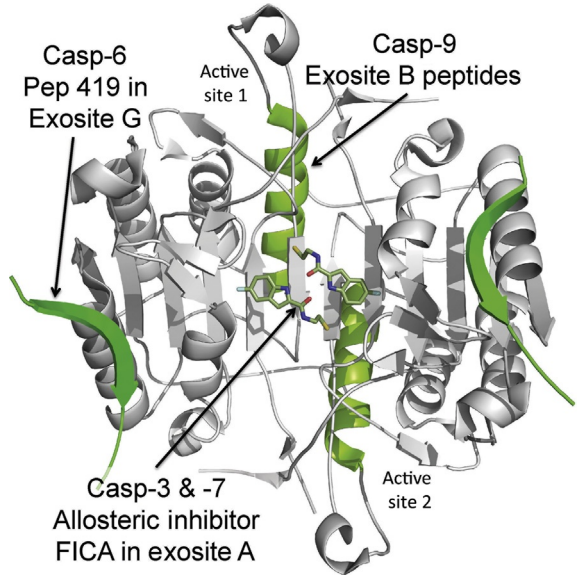

Figure 9.7 Sites for binding of chemical ligands that affect caspase function. The green caspase helix that forms exosite B is highlighted since it is the region that interacts with the BIR3 region of XIAP- and BIR3-derived peptide inhibitors. *Adapted from Velazquez-Delgado (2012) with permission.*

developed at Genentech, which inhibits caspase-6 allosterically (Stanger et al., 2012) (exosite G, Fig. 9.7). Thus, the use of chemical ligands has played a central role in uncovering new mechanisms of allosteric regulation in the caspases as well. Here we describe the methods that have allowed identification and characterization of these allosteric sites.

4.1. Allosteric inhibitors acting at a cavity at the apoptotic caspase dimer interface

The first synthetic allosteric inhibitors of caspases were discovered using a disulfide-tethering approach developed at Sunesis Pharmaceuticals (Erlanson et al., 2000, 2004). Tethering makes use of libraries of monophores (pharmacophores) attached to thiol-containing moieties. The presence of a thiol in each library compound allows formation of a disulfide bond with cysteine residues adjacent to the monophore-binding site. The affinity of the monophore binding to the protein modulates the residence time of the compound on the protein, increasing the likelihood of disulfide bond formation and allowing covalent selection of strongly interacting compounds (Erlanson et al., 2000, 2004). DICA (Fig. 9.8A) was identified using

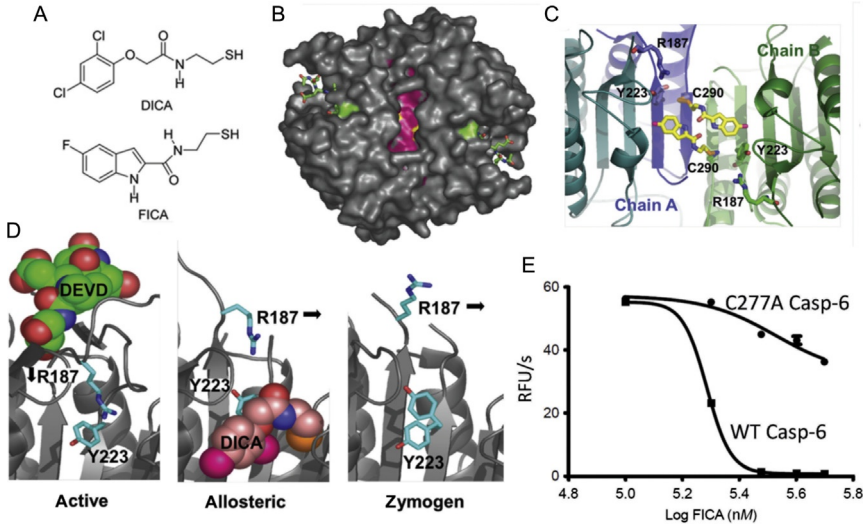

Figure 9.8 Allosteric inhibition at exosite A. (A) The structures of DICA and FICA. (B) The allosteric pocket at the caspase-7 (PDB ID 1F1J) dimer interface exosite A (pink). The FICA/DICA-binding residues C290 on each half of the dimer are shown as yellow patches at the bottom of the pocket. Active sites are denoted by DEVD active-site inhibitor (green sticks) bound to the catalytic cysteine (green patch). (C) The crystal structure of the FICA (yellow) bound caspase-7 exosite A at C290. (D) Conformations of Y233 and R187 shown for active, allosteric inhibitor (DICA, salmon spheres) bound and zymogen caspase-7. DICA bound at the allosteric site prevents R187 and Y233 from pointing down to generate a properly ordered substrate-binding pocket. (E) FICA inhibits wild-type (WT) caspase-6 much more efficiently than C277A caspase-6, indicating that FICA binds and inhibits caspase-6 at the same site and likely by the same mechanism as observed for caspase-7. *Panels A–D are adapted from Hardy et al. (2004a) with permission. Panel E adapted from Velazquez-Delgado (2012) with permission.*

a mass spectrometry-based screen for caspase-3-binding compounds (Hardy et al., 2004a). FICA (Fig. 9.8A) was identified using an apoptosis assay in whole-cell lysates and was found to functionally block cleavage and activation of caspase-3 (Hardy et al., 2004a). Both FICA and DICA control the activity of these caspases by binding specifically in a central cavity at the dimer interface (Fig. 9.8B). The allosteric inhibitors (DICA and FICA) bind covalently to a cysteine (C290 in caspase-7) in the allosteric site (Fig. 9.8C), trapping tyrosine 223 (Y223) in an up position. This conformation of Y223 prevents arginine (R187) from assuming the down conformation, which is required for substrate binding and activity (Fig. 9.8D). The substrate-binding groove in caspases is formed of three loops, L2, L3, and L4 from

one half of the dimer, and L2′ from the other half of the dimer. In the allosterically inhibited forms of caspase-7, L2′ is bound over the allosteric site and thus unable to assist in the assembly of the substrate-binding groove. The relevant conformational changes that lead to allosteric inhibition can be readily visualized in movie form (Hardy, Lam, Nguyen, O'Brien, & Wells, 2004b). Therefore, disruption of the substrate-binding loops is sufficient to lead to inhibition (Hardy & Wells, 2009). Based on sequence and structural homology, we predicted that FICA and DICA would likewise inhibit caspase-6. C290 in caspase-7 is homologous to C277 in caspase-6. FICA inhibits WT caspase-6 but the inhibition is dramatically reduced when the allosteric site thiol (C277) is removed by mutation to alanine (Fig. 9.8E). This demonstrates that the dominant site of inhibition for caspase-6 is C277. Thus, we see that the three prominent apoptotic executioner caspases, caspases-3, -6, and -7, all possess the same allosteric site at the dimer interface.

Two other classes of small molecules that target the same cavity on the dimerization interface of caspases have been identified. Multiring, pyridinyl, copper-containing compounds (Comp-A, -B, -C, and -D), identified by high-throughput screening, act as pan-caspase inhibitors which inactivate both initiators (caspases-2, -8, and -9) and executioners (caspases-3 and -7) with submicromolar IC_{50} values (Feldman et al., 2012). Using Cu anomalous X-ray diffraction similar to that used for caspase-6 inhibition by zinc (Section 2.2) to locate the compounds in caspase-7 crystals, Comp-A was shown to bind at the same location where FICA and DICA bind (exosite A) and cause the active-site loops to be disordered. However, unlike FICA and DICA, Comp-A does not form a covalent bond with C290, thus functioning as a reversible inhibitor. In addition, this exosite A cavity in caspase-8 was shown to noncovalently bind a beta-strand peptidomimetic inhibitor developed at Pfizer (Wang, Watt, et al., 2010). Binding of the inhibitor induced conformational changes in this pocket. Interestingly, because the residues within this pocket are not conserved across caspases, the authors suggested that this site may be amenable to specific targeting of caspase-8. Given our experience with this site (exosite A, Fig. 9.7) which allows inhibition by the same ligands (FICA and DICA) in caspases-3, -6, and -7, we think this site is functionally conserved across caspases. The level of homology in this pocket between caspase-8 and other caspases will likely dictate whether this cavity will indeed be effective for use in a caspase-8-specific manner.

4.2. Rationally designed synthetic peptide allosteric inhibitors mimic XIAP BIR3 dimerization site blocking in caspase-9

Regulation of caspase-9 is distinct from other caspases. Caspase-9 is active only as a dimer (Fig. 9.9A), but can be held in an inactive state by the BIR3 domain of the XIAP protein which blocks dimerization allosterically (Fig. 9.9B). This precise mechanism has not been observed for any other caspase, although it shares some similarities with the interactions of caspase-8 with FLIP (Boatright et al., 2003). Knowing how nature has exploited this allosteric site, we made a set of allosteric inhibitors that mimic

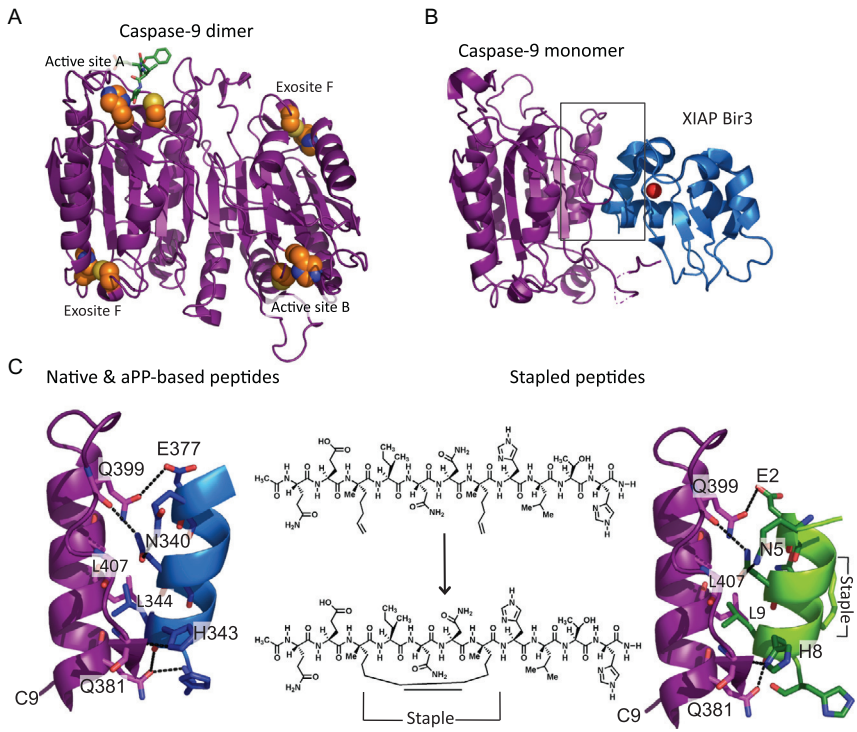

Figure 9.9 Allosteric inhibition of caspase-9 at the dimer interface. (A) Caspase-9 is a dimer composed of A and B chains, each of which has the same amino acid sequence and each possessing the residues required to form one active site. In the structure of mature caspase-9 (PDB ID 1JXQ), only one active site (active site A) is observed in a catalytically competent conformation. Green sticks mark peptide inhibitor in the A-chain active site. For reference, the active site and a zinc-binding exosite F are drawn as orange spheres. (B) XIAP BIR3 domain prevents dimerization and activation of caspase-9 (PDB ID 1NW9). (C) Three classes of BIR3-mimicking peptides produced by novel synthetic schemes developed are shown. *Adapted from Huber et al. (2012) with permission.*

the interaction of XIAP BIR3 with caspase-9 in an effort to develop caspase-9-specific inhibitors. The BIR3 domain has been reported to be conformationally unstable (Shin et al., 2005) so we predicted that it would be necessary to stabilize the α5 helix, which interacts directly with caspase-9, in order to develop potent caspase-9 inhibitors. We engineered three types of stabilized peptides, each designed to remain helical and block caspase-9 dimerization (Fig. 9.9C) (Huber, Ghosh, & Hardy, 2012). We envision that both BIR3 and these peptides compete with caspase-9 monomers for binding the dimerization interface, such that caspase-9 monomers are positive allosteric modulators and BIR3-based peptides are negative allosteric modulators. We built native peptides derived directly from BIR3 and peptides in which caspase-9-interacting residues were grafted on the stable avian pancreatic polypeptide scaffold. For peptides made of native amino acids, we developed an expression and purification method for producing long peptides more quickly and with higher fidelity than chemical synthesis (Huber, Olson, & Hardy, 2009). We also incorporated the nonnative amino acid aminoisobutyric acid, which is α-methylated and enforces peptide helicity in some of the designed peptides. In addition, we synthesized a number of peptides stabilized by an aliphatic "staple" (Fig. 9.9C). We introduced staples 8 and 11 atoms long using nonnative alkenyl amino acids and a ring closing metathesis reaction. All three types of stabilized peptides are helical in solution, in contrast to native peptides, which were not helical. The best inhibitor to date shows a K_i of 16 μ*M*. This level of inhibition by properly folded, helical peptides not only suggests that the entire BIR3 domain is essential for optimal caspase-9 inhibition but also indicates that the dimerization interface of caspase-9 is exploitable as an allosteric site.

Other studies have also targeted this region of the initiator caspases to prevent dimerization. Caspase-9 activated by the apoptosome and an engineered constitutively dimeric caspase-9 were inhibited by small molecules (Comp-A, -B, -C, -D) binding to exosite A at the dimerization interface (Feldman et al., 2012). Active caspase-8 is dimeric, but also exists in equilibrium with its monomeric form, which can be resolved by size-exclusion chromatography. Binding of Comp-A shifted the dimeric caspase-8 to its monomeric form with a concurrent decrease in activity. This is in contrast to caspase-7 which remained dimeric upon binding of Comp-A, although in an inactive, incompetent conformation (Feldman et al., 2012). Thus, it appears that allosteric regulation of dimerization may be uniquely applicable to the initiator caspases which have a low intrinsic dimerization affinity relative to the executioner caspases.

4.3. Synthetic inhibitors of caspase-6

A small peptide, Pep419, developed at Genentech, inhibits caspase-6 allosterically (Stanger et al., 2012) and led to the discovery of exosite G (Fig. 9.7). Pep419 was identified using a phage display screen against caspase-6 zymogen and selectively inhibits caspase-6 function *in vitro* and *in vivo*. Pep419 binds at a novel tetramer interface that centrally involves residue H126 in the binding interface, which is not conserved among executioner caspases. The tetrameric state of caspase-6 zymogen they observed by multiangle light scattering is novel relative to the many reported structures of executioner caspase zymogens as dimers (Chai et al., 2001; Riedl et al., 2001; Wang, Watt, et al., 2010). Pep419 is an allosteric regulator of both active and zymogen caspase-6, which follows a novel noncompetitive mechanism that involves a seemingly global effect on protein dynamics affecting the overall oligomeric state of the enzyme rather than on a specific conformational change. The authors suggest that Pep419 binding stabilizes the tetrameric caspase-6 zymogen form and traps active caspase-6 in that tetrameric, zymogen-like form.

While most reported caspase allosteric inhibitors bind to exosites (Fig. 9.1), a unique uncompetitive, 11 n*M* inhibitor of caspase-6 binds selectively to the enzyme–substrate complex that impedes substrate turnover (Heise et al., 2012). Generated from a chemical optimization screen, compound 3 is an optimized analog of an *N*-furoyl-phenylalanine designed to contain a meta-cyano-substituted D-phenylalanine and a demethylated furan ring. The binding of compound 3 to caspase-6 is dependent on the identity of the peptide substrate and, surprisingly, on the identity of the attached fluorophore. The ternary crystal structure of caspase-6/z-VEID/compound 3 reveals a novel platform for uncompetitive inhibition for any members of the caspase family. This type of inhibition could occur only in the presence of a second small molecule like the fluorophore or in a larger compound composed of both the compound 3 pharmacophore and a fluorophore mimic. Nevertheless, compound 3 and Pep419 provide novel mechanisms for caspase inhibitors that work allosterically or unconventionally.

5. EXPLOITING STRUCTURAL DIFFERENCES AMONG CASPASES

A wealth of structural information is available for all of the apoptotic caspases. These data suggest that the core domain of caspases is highly conserved at a structural level. On the other hand, the prodomains are highly

divergent and very poorly structurally characterized. In addition, at least one apoptotic caspase, caspase-6, can attain a unique helical structure that is unattainable by any other caspase. Structurally unique features are prime for exploitation by allosteric regulators.

5.1. Structural and organizational differences between the apoptotic caspases

Structurally, all caspases contain the highly homologous protease or core domain that is further subdivided into a large (17–20 kDa) and a small (10–12 kDa) subunit that are held together in the zymogen precursor state by an intersubunit linker (ISL). The N-terminus of caspases is a stretch of residues that comprise the prodomain, with the initiator caspases having longer prodomains than the executioners (Fig. 9.10). This difference in prodomain size and structure reflects their respective function in caspase activation. Initiator caspases utilize their prodomains to serve as platforms for protein–protein interactions that are critical during their full activation. Caspase-9 has a caspase activation and recruitment domain (CARD), while caspase-8 contains the death effector domain (DED) to facilitate initial activation. Thus, the CARD and DED are potential targets to inhibit

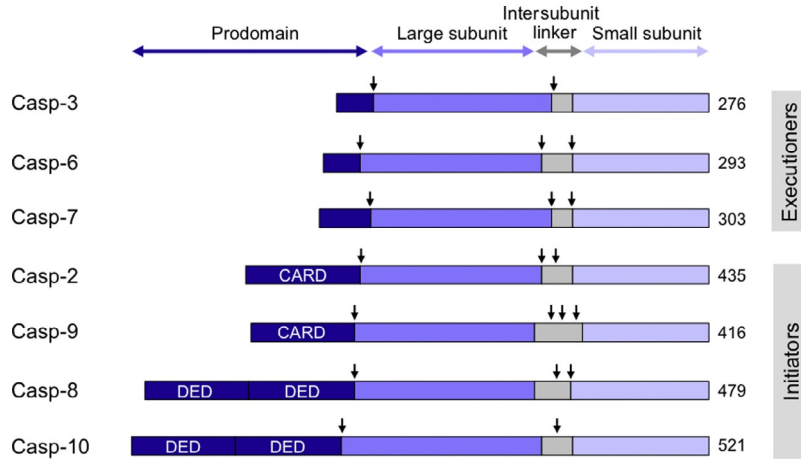

Figure 9.10 Domain organization among the apoptotic caspases. Caspases consist of a prodomain, large subunit, intersubunit linker, and small subunit. Executioner caspases have a short prodomain involved in substrate recognition which has also been proposed to function as a folding chaperone, whereas initiator caspases have a longer prodomain involved in protein:protein interactions. The cleavage sites that lead to production of the mature caspases are indicated by vertical arrows.

initiator caspases. To date, no impact on catalytic function has been attributed to the prodomains of executioner caspases, as prodomain-deleted versions of executioner caspases have been observed to be as active as the full-length protein.

Caspases are synthesized and stored in the zymogen form (procaspase). Cleavage or processing of the ISL as well as dimerization confers maximum activity for caspases (Chai et al., 2001; Pop, Timmer, Sperandio, & Salvesen, 2006; Riedl et al., 2001; Vaidya et al., 2011; Watt et al., 1999; Wilson et al., 1994). Mature, active caspases exist as homodimers. Initiator caspases such as caspases-2, -8, -9, and -10 are monomeric when synthesized (Boatright et al., 2003; Butt, Harvey, Parasivam, & Kumar, 1998; Renatus, Stennicke, Scott, Liddington, & Salvesen, 2001; Wachmann et al., 2010) while executioners dimerize immediately upon ribosome release (Kang, Ko, Kwon, & Choi, 2002; Pop et al., 2001; Talanian et al., 1996). Due to low sequence homology of residues comprising the dimerization interface, the size and nature of the cavity formed at this interface also varies, allowing small molecules to differentially act on this region, whether by preventing the formation of a properly formed active site (e.g., caspase-7; Hardy et al., 2004a) or by inhibiting dimerization (caspases-9; Huber, Ghosh, & Hardy, 2012; Feldman et al., 2012 and -8 Feldman et al., 2012) (see Section 4).

Cleavage of the ISL switches caspases from their inactive to highly active forms. In the case of caspase-9, however, having a longer ISL allows it to facilely support a properly formed active-site loop bundle even prior to cleavage. Wells and colleagues have shown that procaspases-3 and -7, containing short ISLs, can also bind peptide inhibitors and adopt the active conformation even prior to ISL cleavage (Thomsen, Koerber, & Wells, 2013). This suggests that linker cleavage may not be solely a steric requirement but also an allosteric requirement due to the enhanced ability cleaved linker forms the loop bundle which, in turn, stabilizes the active state. In this regard, perhaps the loop bundles themselves could also be considered allosteric sites, although they are proximal to the active site. Almost all caspases have more than one cleavage site in their ISL and the order and pattern of cleavage influences the activity and regulation of the enzyme. In caspase-6, for example, cleavage at D193 occurs before cleavage at D179, as it has been observed that D193A variants are unable to cleave D179 (Vaidya & Hardy, 2011). For caspase-9, the initial cleavage event at D315 generates an epitope that is recognized by the BIR3 domain of XIAP leading to inhibition, while cleavage at D330 by caspase-3 relieves this inhibition (Denault, Eckelman, Shin, Pop, & Salvesen, 2007; Shiozaki et al., 2003; Srinivasula et al., 2001;

Zou et al., 2003). ISL cleavage also plays a role in ubiquitination of caspases, as only cleaved (mature) caspases-9 (Morizane, Honda, Fukami, & Yasuda, 2005) and -8 (Jin et al., 2009), but not their uncleaved zymogen forms are ubiquitinated. We think it is likely that allosteric regulation specific to each caspase will involve exploiting differences in the domain organization of the caspases as discussed here (Fig. 9.10).

5.2. Unique conformation of caspase-6 relative to other caspases

A group at Novartis Pharmaceuticals reported the structure of cleaved (mature) unliganded (apo) caspase-6 (Baumgartner et al., 2009) simultaneous with our determination of the same structures in the presence and absence of the ISL (Vaidya et al., 2011) (Fig. 9.11). All of these structures showed caspase-6 in a conformation that is different than any other caspase structure before or since. Significantly, the 60's and 130's helices were extended, occluding the active site, and the 90's helix is rotated by 21° outward away from the core of the protein (Fig. 9.12). In the past several years, additional structures of caspase-6 in the uncleaved (immature) zymogen (Wang, Cao, et al., 2010) and bound to peptide-based, substrate-like active-site inhibitors have also emerged (Liu, Zhang, Wang, Li, & Su, 2011; Muller, Lamers, Ritchie, Dominguez, et al., 2011; Wang, Cao, et al., 2010) (Fig. 9.11). All of these structures have unique features, particularly in the loops (L1, L2, L3, and L4) which comprise the substrate-binding groove (detailed distinctions noted in Fig. 9.11). An additional structure of apo, mature caspase-6 showed the 130's region in the canonical conformation (Muller, Lamers, Ritchie, Park, et al., 2011) similar to that observed in the zymogen, substrate-bound conformations. This canonical apo mature structure crystallizes at neutral pH, whereas the helical conformation crystallizes at low pH. We have shown that caspase-6 exhibits a helical CD signal at neutral or low pH in the absence of active-site substrate-like ligands and loses ~20% of the helical signal when substrate-like ligands bind, which causes 20% of the helical residues convert to strand or loops (Vaidya et al., 2011). In addition, the fact that the active site of caspase-6 does not bind zinc in solution at neutral or low pH strongly suggests that caspase-6 exists in an equilibrium that favors predominantly the helical conformation at all pHs until substrate binds (Velazquez-Delgado & Hardy, 2012b). Prior to substrate binding, the active-site residues are positioned too far apart to facilitate zinc binding. Together these data lead us to conclude that caspase-6 is capable of interconverting between the helical conformation

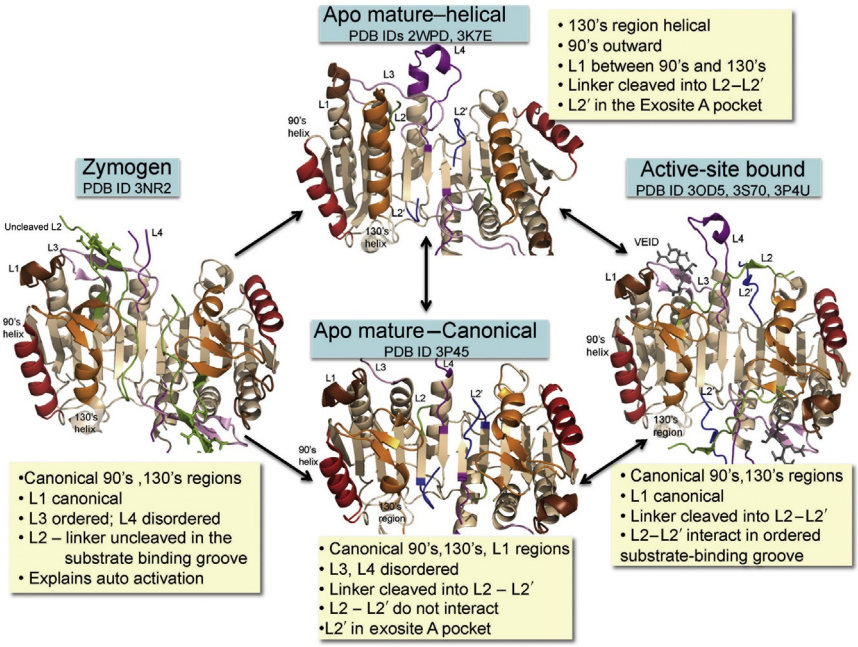

Figure 9.11 Conformational changes during caspase-6 lifecycle. Crystal structures of the caspase-6 are available for zymogen, mature and active-site bound forms. The zymogen of caspase-6 exists in a conformation that explains the structural basis of self-processing. The mature form exists in a conformational equilibrium between a helical and a canonical conformation, though in the canonical conformation far more regions of the protein are disordered. The equilibrium seems to favor the helical form at all pHs. The active-site bound form attains a structure that is extremely similar to all other active-site bound caspases. The colored regions highlight conformational changes that occur during the transitions between these states in the 90's helix (red), 130's region (orange), L1 loop (brown), L2 (green), L2′ (blue), L3 pink, and L4 (purple). Significant structural characteristics are denoted for each conformation (yellow boxes).

and the canonical conformation, but that caspase-6 exists predominantly in the helical conformation in solution.

The helical conformation (Fig. 9.12, orange) is of interest because it cannot bind substrate and is thus naturally inactive. This helical conformation cannot be adopted by any other caspase (Vaidya & Hardy, 2011). This is because caspase-6 is the only caspase lacking helix-breaking glycine and proline residues in this region, so it is the only caspase that can form an extended 130's helix (Vaidya & Hardy, 2011). Thus, the helical conformation appears to be unique to caspase-6. Any allosteric sites that exist in the helical

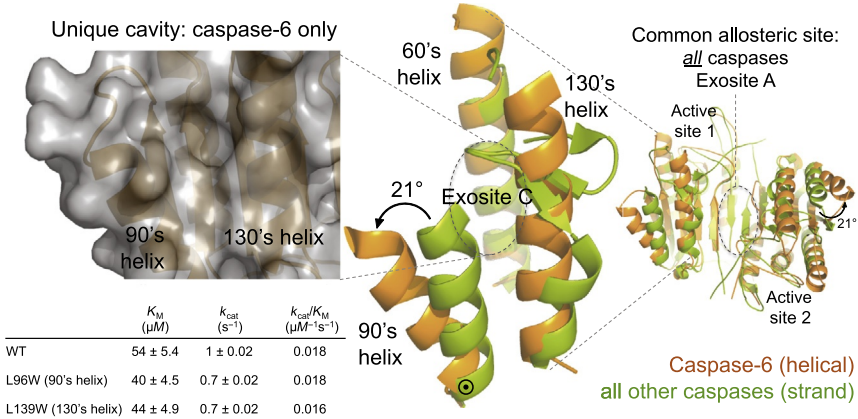

	K_M (μM)	k_{cat} (s^{-1})	k_{cat}/K_M ($\mu M^{-1}s^{-1}$)
WT	54 ± 5.4	1 ± 0.02	0.018
L96W (90's helix)	40 ± 4.5	0.7 ± 0.02	0.018
L139W (130's helix)	44 ± 4.9	0.7 ± 0.02	0.016
L96W/L139W	47 ± 2.0	$4.6 \pm 4.2 \times 10^{-3}$	9.8×10^{-5}

Figure 9.12 Caspase-6 (orange, PDB ID 3NKF) exists in an extended helical conformation that cannot be attained by any other caspase, which all have the same canonical strand structure as caspase-7 (green, PDB ID 1F1J) in the 90's helix. A cavity formed when the 90's helix rotates away from the 130's helix can function as a unique allosteric site at exosite C, as shown by insertion of tryptophan residues designed to hold the 90's helix in an open conformation. *Adapted from Vaidya et al. (2011) with permission.*

conformation but not in the canonical conformation should be extremely specific for caspase-6. We have identified one such potentially exploitable cavity (exosite C, Fig. 9.12). When residues in the 90's and 130's helices were replaced by tryptophan (L96W/L139W), the enzyme was locked in the helical conformation and was allosterically inactivated (Fig. 9.12, table). We have noted a marked circular dichroism signal in this helical state, which also serves as a robust spectroscopic signature for this unique, inactivated state (Vaidya et al., 2011), enabling identification of inhibitors that bind to the helical conformation.

5.3. Caspase allostery identified by mutagenesis

Savvy use of mutagenesis has also pinpointed allosterically sensitive sites in caspases. Clark and his group have shown that variants at dimer interface residue V266 exploit caspase-3 allostery. V266 is extremely sensitive in maintaining the dimeric state, and thus the conformation and catalytic function of caspase-3. The glutamate variant V266E in mature caspase-3 shows a lower activity and efficiency of apoptotic death than WT. Intriguingly, the V266E variant was also observed to have intrinsic activity even in an uncleavable version of procaspase-3 (D9A/D28A/D175A) (Walters

et al., 2009), which shows an extremely low catalytic efficiency for the WT (V266) version (Bose, Pop, Feeney, & Clark, 2003). This suggests that V266E is capable of activating caspase-3 even before caspase-3 is processed. The authors propose that the negative charge of E266 disrupts the original hydrophobic cluster across the dimer interface and that a specified series of conformational changes in the loops allow the correct orientation of the catalytic and substrate-binding residues (Walters et al., 2009). In particular, the V266E mutation forces the ISL to an active position forming the substrate-binding pocket and loop bundle. This mechanistic suggestion is supported by the structure of procaspase-7 (Riedl et al., 2001) and by a recently published structure of WT procaspase-3 (Thomsen et al., 2013). In this structure, although the ISL is partially disordered, the residues (K186–V189) substantially shift to the dimer interface, confirming that the central cavity is blocked by the uncleaved linker. In addition, another crucial loop LH, which is parallel with loop 3, appears to be expelled out of the central cavity in the inactive WT procaspase-3. During the procaspase-3 activation by V266E, LH might also require an insertion into the relieved central cavity, similar to the motion of the L3 loop, for the active orientation of catalytic residue H121. Interestingly, a different variant at the same position, V266H, inhibits mature caspase-3 activity because it could prevent R164 and the L2 loop from inserting into the central cavity and thus increase the population of the inactive ensemble (Walters et al., 2009; Walters, Schipper, Swartz, Mattos, & Clark, 2012). Thus, it is clear based on these mutational and structural analyses that this region of the protein, overlapping with exosite A, is an allosterically modulatable region. This is significant because the same site has been identified by both mutagenesis and a number of small-molecule ligands, suggesting that mutagenesis alone can be very predictive of allosteric sites.

5.4. Exosites for substrate recognition in caspases

Proteases require precise cleavage instructions to suppress potentially devastating and irreversible effects. One effective method for cleavage control is through extremely selective sequence recognition, where only specific combinations of residues are recognized at the active site and cleaved by the protease. In addition to this, proteases have also evolved exosites that allow for further exclusivity of substrates as well as increasing the rate of catalysis. Thrombin is a prominent example of a protease that utilizes exosites to perform its many duties in the coagulation cascade (for review,

see Huntington, 2005; Lane, Philippou, & Huntington, 2005). Exosites on the surface of thrombin are recognized by various substrates and cofactors that decide its ultimate fate (Stubbs & Bode, 1995; Verhamme, Olson, Tollefsen, & Bock, 2002).

It now appears clear that caspases also use exosites to increase efficiency of catalysis and improve selectivity for substrates. As the cell undergoes apoptosis, it is imperative that the active caspases carry out their duties swiftly and accurately to ensure a clean death. Two substrates, poly(ADP ribose)polymerase 1 (PARP) and p23, are critical apoptotic caspase targets. Both of these substrates are primarily cleaved by caspase-7, yet their cleavage site shares a recognition sequence for caspase-3, which has a much higher intrinsic activity than caspase-7. The Denault group discovered that caspase-7 predominately cleaves these substrates due to a charged exosite near the N-terminus of the protein. Four consecutive lysine residues create a basic patch that allows for caspase-7, the slower executioner, to selectively cleave PARP much more efficiently than caspase-3. Removal of the caspase-7 prodomain is essential for engaging this exosite, providing a first glimpse of the role of prodomain removal in the executioner caspases.

Discovery of this exosite indicates that caspase-7 requires more than just a consensus cleavage motif in the substrate to attain full specificity. Due to the sensitive nature of apoptosis and similarities across the caspase family, we hypothesize that other caspases likewise contain exosites that aid in achieving full proteolytic specificity. If these sites resemble the caspase-7 exosite, then they too may be distant from the active site. Discovery of these allosteric regions offers tremendous potential for precise control of individual caspases in both apoptotic and nonapoptotic functions.

6. FUTURE OF ALLOSTERIC SITE DISCOVERY

Work from a large number of labs has contributed and will continue to contribute to a global map of apoptotic caspase allostery. In the current map of caspase allostery (Fig. 9.1), important trends are already emerging. For example, the fact that chemical ligands, phosphorylation, and zinc all exploit the F/G region suggests that this region is important in controlling the function of multiple caspases. On the other hand, we have shown that exosite C is only present in caspase-6 (Fig. 9.1). Thus, the A or F/G exosite should be exploited to control caspases globally and the C exosite would be appropriate for inhibiting caspase-6 selectively. As we expand and improve our map of caspase allostery, we will identify regions that play critical roles in

caspase function, improve our understanding of natural methods of regulation: phosphorylation and other PTMs as well as binding of zinc and other metals. This continued understanding will thus increase our chances for strategic control of apoptosis.

The methods outlined in this chapter are of interest because they can be undertaken by a wide number of groups. In a similar manner to the approach described here for the apoptotic caspases, any other family of proteins could likewise be studied. Several obvious approaches remain to be undertaken in the study of the apoptotic caspases. In addition to zinc, any other metals capable of inhibiting caspases could be used with anomalous diffraction to unambiguously identify the binding sites. Coupling this with a mutagenesis approach is a rapid way to confirm the binding site and determine whether the site is an allosteric inhibitory site. Whereas this chapter has focused on work in the apoptotic caspases, a full understanding of this class of enzymes requires comparative work with the inflammatory caspases and less functionally well-characterized caspases including caspase-2.

The most important outcome of this type of work in the future will be the ability to assess which type of inhibition (orthosteric vs. various allosteric sites) is most effective and specific. These results will also address the important hypothesis that engaging different allosteric regulatory mechanism will impact only certain subsets of caspase function. Confirming that certain kinds of inhibition (e.g. zinc vs. phosphorylation) result in unique cellular outcomes will allow development of new caspase-directed drugs that will likely avoid the problems with toxicity that have plagued caspase inhibitors in the clinic to date.

ACKNOWLEDGMENTS

S. J. E. was supported by NSF Grant IGERT DGE-0654128. B. P. S. was supported in part by National Research Service Award T32 GM08515 from the National Institute of Health. This work was supported by the National Institutes of Health GM80532.

REFERENCES

Allan, L. A., & Clarke, P. R. (2007). Phosphorylation of caspase-9 by CDK1/cyclin B1 protects mitotic cells against apoptosis. *Molecular Cell*, *26*(2), 301–310.

Allan, L. A., Morrice, N., Brady, S., Magee, G., Pathak, S., & Clarke, P. R. (2003). Inhibition of caspase-9 through phosphorylation at Thr 125 by ERK MAPK. *Nature Cell Biology*, *5*(7), 647–654.

Alvarado-Kristensson, M., Melander, F., Leandersson, K., Ronnstrand, L., Wernstedt, C., & Andersson, T. (2004). p38-MAPK signals survival by phosphorylation of caspase-8 and caspase-3 in human neutrophils. *Journal of Experimental Medicine*, *199*(4), 449–458.

Baumgartner, R., Meder, G., Briand, C., Decock, A., D'arcy, A., Hassiepen, U., et al. (2009). The crystal structure of caspase-6, a selective effector of axonal degeneration. *Biochemistry Journal*, *423*, 429–439.

Boatright, K. M., Renatus, M., Scott, F. L., Sperandio, S., Shin, H., Pedersen, I. M., et al. (2003). A unified model for apical caspase activation. *Molecular Cell*, *11*(2), 529–541.

Bose, K., Pop, C., Feeney, B., & Clark, A. C. (2003). An uncleavable procaspase-3 mutant has a lower catalytic efficiency but an active site similar to that of mature caspase-3. *Biochemistry*, *42*(42), 12298–12310.

Boucher, D., Blais, V., & Denault, J. B. (2012). Caspase-7 uses an exosite to promote poly(ADP ribose) polymerase 1 proteolysis. *Proceedings of the National Academy of Sciences of the United States of America*, *109*(15), 5669–5674.

Bozym, R. A., Thompson, R. B., Stoddard, A. K., & Fierke, C. A. (2006). Measuring picomolar intracellular exchangeable zinc in PC-12 cells using a ratiometric fluorescence biosensor. *ACS Chemical Biology*, *1*(2), 103–111.

Butt, A. J., Harvey, N. L., Parasivam, G., & Kumar, S. (1998). Dimerization and autoprocessing of the Nedd2 (caspase-2) precursor requires both the prodomain and the carboxyl-terminal regions. *The Journal of Biological Chemistry*, *273*(12), 6763–6768.

Cao, Q., Wang, X. J., Liu, C. W., Liu, D. F., Li, L. F., Gao, Y. Q., et al. (2012). Inhibitory mechanism of caspase-6 phosphorylation revealed by crystal structures, molecular dynamics simulations, and biochemical assays. *The Journal of Biological Chemistry*, *287*(19), 15371–15379.

Carter, J. E., Truong-Tran, A. Q., Grosser, D., Ho, L., Ruffin, R. E., & Zalewski, P. D. (2002). Involvement of redox events in caspase activation in zinc-depleted airway epithelial cells. *Biochemical and Biophysical Research Communications*, *297*(4), 1062–1070.

Chai, J., Wu, Q., Shiozaki, E., Srinivasula, S. M., Alnemri, E. S., & Shi, Y. (2001). Crystal structure of a procaspase-7 zymogen: Mechanisms of activation and substrate binding. *Cell*, *107*(3), 399–407.

Chimienti, F., Seve, M., Richard, S., Mathieu, J., & Favier, A. (2001). Role of cellular zinc in programmed cell death: Temporal relationship between zinc depletion, activation of caspases, and cleavage of Sp family transcription factors. *Biochemical Pharmacology*, *62*(1), 51–62.

Datta, D., Scheer, J. M., Romanowski, M. J., & Wells, J. A. (2008). An allosteric circuit in caspase-1. *Journal of Molecular Biology*, *381*(5), 1157–1167.

Denault, J. B., Drag, M., Salvesen, G. S., Alves, J., Heidt, A. B., Deveraux, Q., et al. (2007). Small molecules not direct activators of caspases. *Nature Chemical Biology*, *3*(9), 519, author reply 520.

Denault, J. B., Eckelman, B. P., Shin, H., Pop, C., & Salvesen, G. S. (2007). Caspase 3 attenuates XIAP (X-linked inhibitor of apoptosis protein)-mediated inhibition of caspase 9. *Biochemistry Journal*, *405*(1), 11–19.

Dimmeler, S., Haendeler, J., Nehls, M., & Zeiher, A. M. (1997). Suppression of apoptosis by nitric oxide via inhibition of interleukin-1beta-converting enzyme (ICE)-like and cysteine protease protein (CPP)-32-like proteases. *Journal of Experimental Medicine*, *185*(4), 601–607.

Dix, M. M., Simon, G. M., Wang, C., Okerberg, E., Patricelli, M. P., & Cravatt, B. F. (2012). Functional interplay between caspase cleavage and phosphorylation sculpts the apoptotic proteome. *Cell*, *150*(2), 426–440.

Duncan, J. S., Turowec, J. P., Duncan, K. E., Vilk, G., Wu, C., Luscher, B., et al. (2011). A peptide-based target screen implicates the protein kinase CK2 in the global regulation of caspase signaling. *Science Signaling*, *4*(172), ra30.

Erlanson, D. A., Braisted, A. C., Raphael, D. R., Randal, M., Stroud, R. M., Gordon, E. M., et al. (2000). Site-directed ligand discovery. *Proceedings of the National Academy of Sciences of the United States of America*, *97*(17), 9367–9372.

Erlanson, D. A., Wells, J. A., & Braisted, A. C. (2004). Tethering: Fragment-based drug discovery. *Annual Review of Biophysics and Biomolecular Structure*, *33*, 199–223.
Feldman, T., Kabaleeswaran, V., Jang, S. B., Antczak, C., Djaballah, H., Wu, H., et al. (2012). A class of allosteric caspase inhibitors identified by high-throughput screening. *Molecular Cell*, *47*(4), 585–595.
Fukada, T., & Kambe, T. (2011). Molecular and genetic features of zinc transporters in physiology and pathogenesis. *Metallomics*, *3*(7), 662–674.
Hardy, J. A., Lam, J., Nguyen, J. T., O'Brien, T., & Wells, J. A. (2004). Discovery of an allosteric site in the caspases. *Proceedings of the National Academy of Sciences of the United States of America*, *101*(34), 12461.
Hardy, J. A., Lam, J., Nguyen, J. T., O'Brien, T., & Wells, J. A. (2004b). http://www.pnas.org/content/suppl/2004/08/09/0404781101.DC1/04781Movie2.mov.
Hardy, J. A., & Wells, J. A. (2004). Searching for new allosteric sites in enzymes. *Current Opinion in Structural Biology*, *14*(6), 706–715.
Hardy, J. A., & Wells, J. A. (2009). Dissecting an allosteric switch in caspase-7 using chemical and mutational probes. *The Journal of Biological Chemistry*, *284*(38), 26063.
Hayashi, N., Shirakura, H., Uehara, T., & Nomura, Y. (2006). Relationship between SUMO-1 modification of caspase-7 and its nuclear localization in human neuronal cells. *Neuroscience Letters*, *397*(1–2), 5–9.
Heise, C. E., Murray, J., Augustyn, K. E., Bravo, B., Chugha, P., Cohen, F., et al. (2012). Mechanistic and structural understanding of uncompetitive inhibitors of caspase-6. *PLoS One*, *7*(12), e50864.
Huang, Z., Pinto, J. T., Deng, H., & Richie, J. P., Jr. (2008). Inhibition of caspase-3 activity and activation by protein glutathionylation. *Biochemical Pharmacology*, *75*(11), 2234–2244 [Research Support, N.I.H., Extramural].
Huber, K. L., Ghosh, S., & Hardy, J. A. (2012). Inhibition of caspase-9 by stabilized peptides targeting the dimerization interface. *Biopolymers Peptide Science*, *98*(5), 451–465.
Huber, K. L., & Hardy, J. A. (2012). Mechanism of zinc-mediated inhibition of caspase-9. *Protein Sciences*, *20*(7), 1056–1065.
Huber, K. L., Olson, K. D., & Hardy, J. A. (2009). Robust production of a peptide library using methodological synchronization. *Protein Expression and Purification*, *67*(2), 139–147.
Huntington, J. A. (2005). Molecular recognition mechanisms of thrombin. *Journal of Thrombosis and Haemostasis*, *3*(8), 1861–1872.
Jia, S. H., Parodo, J., Kapus, A., Rotstein, O. D., & Marshall, J. C. (2008). Dynamic regulation of neutrophil survival through tyrosine phosphorylation or dephosphorylation of caspase-8. *The Journal of Biological Chemistry*, *283*(9), 5402–5413.
Jin, Z., Li, Y., Pitti, R., Lawrence, D., Pham, V. C., Lill, J. R., et al. (2009). Cullin3-based polyubiquitination and p62-dependent aggregation of caspase-8 mediate extrinsic apoptosis signaling. *Cell*, *137*(4), 721–735.
Kang, B. H., Ko, E., Kwon, O. K., & Choi, K. Y. (2002). The structure of procaspase 6 is similar to that of active mature caspase 6. *Biochemistry Journal*, *364*(Pt. 3), 629–634.
Kim, Y. M., Talanian, R. V., & Billiar, T. R. (1997). Nitric oxide inhibits apoptosis by preventing increases in caspase-3-like activity via two distinct mechanisms. *The Journal of Biological Chemistry*, *272*(49), 31138–31148.
Kohler, J. E., Dubach, J. M., Naik, H. B., Tai, K., Blass, A. L., & Soybel, D. I. (2010). Monochloramine-induced toxicity and dysregulation of intracellular Zn2+ in parietal cells of rabbit gastric glands. *American Journal of Physiology—Gastrointestinal and Liver Physiology*, *299*(1), G170–G178.
Kohler, J. E., Mathew, J., Tai, K., Blass, A. L., Kelly, E., & Soybel, D. I. (2009). Monochloramine impairs caspase-3 through thiol oxidation and Zn2+ release. *Journal of Surgical Research*, *153*(1), 121–127.

Krezel, A., Hao, Q., & Maret, W. (2007). The zinc/thiolate redox biochemistry of metallothionein and the control of zinc ion fluctuations in cell signaling. *Archives of Biochemistry and Biophysics*, *463*(2), 188–200.

Krezel, A., & Maret, W. (2006). Zinc-buffering capacity of a eukaryotic cell at physiological pZn. *Journal of Biological Inorganic Chemistry*, *11*(8), 1049–1062.

Kurokawa, M., & Kornbluth, S. (2009). Caspases and kinases in a death grip. *Cell*, *138*(5), 838–854.

Lai, Y. C., Pan, K. T., Chang, G. F., Hsu, C. H., Khoo, K. H., Hung, C. H., et al. (2011). Nitrite-mediated S-nitrosylation of caspase-3 prevents hypoxia-induced endothelial barrier dysfunction. *Circulation Research*, *109*(12), 1375–1386.

Lane, D. A., Philippou, H., & Huntington, J. A. (2005). Directing thrombin. *Blood*, *106*(8), 2605–2612.

Leyva, M. J., Degiacomo, F., Kaltenbach, L. S., Holcomb, J., Zhang, N., Gafni, J., et al. (2010). Identification and evaluation of small molecule pan-caspase inhibitors in Huntington's disease models. *Chemistry & Biology*, *17*(11), 1189–1200.

Li, J., Billiar, T. R., Talanian, R. V., & Kim, Y. M. (1997). Nitric oxide reversibly inhibits seven members of the caspase family via S-nitrosylation. *Biochemical and Biophysical Research Communications*, *240*(2), 419–424.

Li, X., Wen, W., Liu, K., Zhu, F., Malakhova, M., Peng, C., et al. (2011). Phosphorylation of caspase-7 by p21-activated protein kinase (PAK) 2 inhibits chemotherapeutic drug-induced apoptosis of breast cancer cell lines. *The Journal of Biological Chemistry*, *286*(25), 22291–22299.

Liu, X., Zhang, H., Wang, X. J., Li, L. F., & Su, X. D. (2011). Get phases from arsenic anomalous scattering: De novo SAD phasing of two protein structures crystallized in cacodylate buffer. *PLoS One*, *6*(9), e24227.

Lopez-Otin, C., & Hunter, T. (2010). The regulatory crosstalk between kinases and proteases in cancer. *Nature Reviews Cancer*, *10*(4), 278–292.

Minguez, P., Parca, L., Diella, F., Mende, D. R., Kumar, R., Helmer-Citterich, M., et al. (2012). Deciphering a global network of functionally associated post-translational modifications. *Molecular Systems Biology*, *8*, 599.

Morizane, Y., Honda, R., Fukami, K., & Yasuda, H. (2005). X-linked inhibitor of apoptosis functions as ubiquitin ligase toward mature caspase-9 and cytosolic Smac/DIABLO. *The Journal of Biochemistry*, *137*(2), 125–132.

Muller, I., Lamers, M. B., Ritchie, A. J., Dominguez, C., Munoz-Sanjuan, I., & Kiselyov, A. (2011). Structure of human caspase-6 in complex with Z-VAD-FMK: New peptide binding mode observed for the non-canonical caspase conformation. *Bioorganic and Medicinal Chemistry Letters*, *21*(18), 5244–5247.

Muller, I., Lamers, M. B., Ritchie, A. J., Park, H., Dominguez, C., Munoz-Sanjuan, I., et al. (2011). A new apo-caspase-6 crystal form reveals the active conformation of the apoenzyme. *Journal of Molecular Biology*, *410*(2), 307–315.

Perry, D. K., Smyth, M. J., Stennicke, H. R., Salvesen, G. S., Duriez, P., Poirier, G. G., et al. (1997). Zinc is a potent inhibitor of the apoptotic protease, caspase-3. A novel target for zinc in the inhibition of apoptosis. *The Journal of Biological Chemistry*, *272*(30), 18530–18533.

Peterson, Q. P., Goode, D. R., West, D. C., Ramsey, K. N., Lee, J. J., & Hergenrother, P. J. (2009). PAC-1 activates procaspase-3 in vitro through relief of zinc-mediated inhibition. *Journal of Molecular Biology*, *388*(1), 144–158.

Pop, C., Chen, Y. R., Smith, B., Bose, K., Bobay, B., Tripathy, A., et al. (2001). Removal of the pro-domain does not affect the conformation of the procaspase-3 dimer. *Biochemistry*, *40*(47), 14224–14235.

Pop, C., Timmer, J., Sperandio, S., & Salvesen, G. S. (2006). The apoptosome activates caspase-9 by dimerization. *Molecular Cell*, *22*(2), 269–275.

Raina, D., Pandey, P., Ahmad, R., Bharti, A., Ren, J., Kharbanda, S., et al. (2005). c-Abl tyrosine kinase regulates caspase-9 autocleavage in the apoptotic response to DNA damage. *The Journal of Biological Chemistry*, *280*(12), 11147–11151.

Renatus, M., Stennicke, H. R., Scott, F. L., Liddington, R. C., & Salvesen, G. S. (2001). Dimer formation drives the activation of the cell death protease caspase 9. *Proceedings of the National Academy of Sciences of the United States of America*, *98*(25), 14250.

Riedl, S. J., Fuentes-Prior, P., Renatus, M., Kairies, N., Krapp, S., Huber, R., et al. (2001). Structural basis for the activation of human procaspase-7. *Proceedings of the National Academy of Sciences of the United States of America*, *98*(26), 14790.

Scheer, J. M., Romanowski, M. J., & Wells, J. A. (2006). A common allosteric site and mechanism in caspases. *Proceedings of the National Academy of Sciences of the United States of America*, *103*(20), 7595–7600.

Schrantz, N., Auffredou, M. T., Bourgeade, M. F., Besnault, L., Leca, G., & Vazquez, A. (2001). Zinc-mediated regulation of caspases activity: Dose-dependent inhibition or activation of caspase-3 in the human Burkitt lymphoma B cells (Ramos). *Cell Death and Differentiation*, *8*(2), 152–161.

Seet, B. T., Dikic, I., Zhou, M. M., & Pawson, T. (2006). Reading protein modifications with interaction domains. *Nature Reviews. Molecular Cell Biology*, *7*(7), 473–483.

Seifert, A., Allan, L. A., & Clarke, P. R. (2008). DYRK1A phosphorylates caspase 9 at an inhibitory site and is potently inhibited in human cells by harmine. *The FEBS Journal*, *275*(24), 6268–6280.

Shin, H., Renatus, M., Eckelman, B. P., Nunes, V. A., Sampaio, C. A., & Salvesen, G. S. (2005). The BIR domain of IAP-like protein 2 is conformationally unstable: Implications for caspase inhibition. *Biochemistry Journal*, *385*(Pt. 1), 1–10.

Shiozaki, E. N., Chai, J., Rigotti, D. J., Riedl, S. J., Li, P., Srinivasula, S. M., et al. (2003). Mechanism of XIAP-mediated inhibition of caspase-9. *Molecular Cell*, *11*(2), 519–527.

Srinivasula, S. M., Hegde, R., Saleh, A., Datta, P., Shiozaki, E., Chai, J., et al. (2001). A conserved XIAP-interaction motif in caspase-9 and Smac/DIABLO regulates caspase activity and apoptosis. *Nature*, *410*(6824), 112–116.

Stanger, K., Steffek, M., Zhou, L., Pozniak, C. D., Quan, C., Franke, Y., et al. (2012). Allosteric peptides bind a caspase zymogen and mediate caspase tetramerization. *Nature Chemical Biology*, *8*(7), 655–660.

Stennicke, H. R., & Salvesen, G. S. (1997). Biochemical characteristics of caspases-3, -6, -7, and -8. *The Journal of Biological Chemistry*, *272*(41), 25719.

Stubbs, M. T., & Bode, W. (1995). The clot thickens: Cues provided by thrombin structure. *Trends in Biochemical Sciences*, *20*(1), 23–28.

Suzuki, A., Kusakai, G., Kishimoto, A., Shimojo, Y., Miyamoto, S., Ogura, T., et al. (2004). Regulation of caspase-6 and FLIP by the AMPK family member ARK5. *Oncogene*, *23*(42), 7067–7075.

Talanian, R. V., Dang, L. C., Ferenz, C. R., Hackett, M. C., Mankovich, J. A., Welch, J. P., et al. (1996). Stability and oligomeric equilibria of refolded interleukin-1beta converting enzyme. *The Journal of Biological Chemistry*, *271*(36), 21853–21858.

Thomsen, N. D., Koerber, J. T., & Wells, J. A. (2013). Structural snapshots reveal distinct mechanisms of procaspase-3 and -7 activation. *Proceedings of the National Academy of Sciences of the United States of America*, *110*(21), 8477–8482.

Truong-Tran, A. Q., Grosser, D., Ruffin, R. E., Murgia, C., & Zalewski, P. D. (2003). Apoptosis in the normal and inflamed airway epithelium: Role of zinc in epithelial protection and procaspase-3 regulation. *Biochemical Pharmacology*, *66*(8), 1459–1468.

Vaidya, S., & Hardy, J. A. (2011). Caspase-6 latent state stability relies on helical propensity. *Biochemistry*, *50*(16), 3282–3287.

Vaidya, S., Velazquez-Delgado, E. M., Abbruzzese, G., & Hardy, J. A. (2011). Substrate-induced conformational changes occur in all cleaved forms of caspase-6. *Journal of Molecular Biology*, *406*(1), 75–91.

Velazquez-Delgado, E. M. (2012). *Allosteric regulation of caspase-6 proteolytic activity*. Amherst: University of Massachusetts, unpublished dissertation.

Velazquez-Delgado, E. M., & Hardy, J. A. (2012a). Phosphorylation regulates assembly of the caspase-6 substrate-binding groove. *Structure*, *20*(4), 742–751.

Velazquez-Delgado, E. M., & Hardy, J. A. (2012b). Zinc-mediated allosteric inhibition of caspase-6. *The Journal of Biological Chemistry*, *287*(43), 36000–36011.

Verhamme, I. M., Olson, S. T., Tollefsen, D. M., & Bock, P. E. (2002). Binding of exosite ligands to human thrombin. Re-evaluation of allosteric linkage between thrombin exosites I and II. *TheJournal of Biological Chemistry*, *277*(9), 6788–6798.

Wachmann, K., Pop, C., van Raam, B. J., Drag, M., Mace, P. D., Snipas, S. J., et al. (2010). Activation and specificity of human caspase-10. *Biochemistry*, *49*(38), 8307–8315.

Walters, J., Pop, C., Scott, F. L., Drag, M., Swartz, P., Mattos, C., et al. (2009). A constitutively active and uninhibitable caspase-3 zymogen efficiently induces apoptosis. *Biochemistry Journal*, *424*(3), 335–345.

Walters, J., Schipper, J. L., Swartz, P., Mattos, C., & Clark, A. C. (2012). Allosteric modulation of caspase 3 through mutagenesis. *Bioscience Reports*, *32*(4), 401–411.

Wang, X. J., Cao, Q., Liu, X., Wang, K. T., Mi, W., Zhang, Y., et al. (2010). Crystal structures of human caspase 6 reveal a new mechanism for intramolecular cleavage self-activation. *EMBO Reports*, *11*(11), 841–847.

Wang, Z., Watt, W., Brooks, N. A., Harris, M. S., Urban, J., Boatman, D., et al. (2010). Kinetic and structural characterization of caspase-3 and caspase-8 inhibition by a novel class of irreversible inhibitors. *Biochimica et Biophysica Acta*, *1804*(9), 1817–1831.

Watt, W., Koeplinger, K. A., Mildner, A. M., Heinrikson, R. L., Tomasselli, A. G., & Watenpaugh, K. D. (1999). The atomic-resolution structure of human caspase-8, a key activator of apoptosis. *Structure*, *7*(9), 1135–1143.

Wilson, K. P., Black, J. A., Thomson, J. A., Kim, E. E., Griffith, J. P., Navia, M. A., et al. (1994). Structure and mechanism of interleukin-1 beta converting enzyme. *Nature*, *370*(6487), 270–275.

Witkowski, W. A., & Hardy, J. A. (2011). A designed redox-controlled caspase. *Protein Sciences*, *20*(8), 1421–1431.

Yoo, N. J., Lee, S. H., Jeong, E. G., & Lee, S. H. (2007). Expression of phosphorylated caspase-9 in gastric carcinomas. *APMIS*, *115*(4), 354–359 [Research Support, Non-U.S. Gov't].

Zalewski, P. D., Forbes, I. J., & Betts, W. H. (1993). Correlation of apoptosis with change in intracellular labile Zn(II) using zinquin [(2-methyl-8-p-toluenesulphonamido-6-quinolyloxy)acetic acid], a new specific fluorescent probe for Zn(II). *Biochemistry Journal*, *296*(Pt. 2), 403–408.

Zou, H., Yang, R., Hao, J., Wang, J., Sun, C., Fesik, S. W., et al. (2003). Regulation of the Apaf-1/caspase-9 apoptosome by caspase-3 and XIAP. *The Journal of Biological Chemistry*, *278*(10), 8091–8098.